SOLAR PHYSICS

Generation of solar spicules and subsequent atmospheric heating

Tanmoy Samanta¹, Hui Tian¹*, Vasyl Yurchyshyn², Hardi Peter³, Wenda Cao², Alphonse Sterling⁴, Robertus Erdélyi^{5,6}, Kwangsu Ahn², Song Feng⁷, Dominik Utz⁸, Dipankar Banerjee⁹, Yajie Chen¹

Spicules are rapidly evolving fine-scale jets of magnetized plasma in the solar chromosphere. It remains unclear how these prevalent jets originate from the solar surface and what role they play in heating the solar atmosphere. Using the Goode Solar Telescope at the Big Bear Solar Observatory, we observed spicules emerging within minutes of the appearance of opposite-polarity magnetic flux around dominant-polarity magnetic field concentrations. Data from the Solar Dynamics Observatory showed subsequent heating of the adjacent corona. The dynamic interaction of magnetic fields (likely due to magnetic reconnection) in the partially ionized lower solar atmosphere appears to generate these spicules and heat the upper solar atmosphere.

olar spicules are small-scale, jet-like plasma features observed ubiquitously in the solar chromosphere, the interface between the visible surface (photosphere) of the Sun and its hot outer atmosphere (corona) (1–4). Spicules may play a role in the supply of energy and material to the corona and solar wind (4, 5). They often have lifetimes ranging from 1 to 12 min and are characterized by rising and falling motions with speeds of 15 to 40 km s⁻¹ (1, 6). Some spicules may have apparent speeds of ~100 km s⁻¹ and

lifetimes less than 1 min (7). In on-disk observations of the chromosphere, these spicules often appear as elongated, short-lived dark structures (8). Some spicules are heated to \geq 100,000 K (9, 10).

Theoretical models of spicules have included driving by shock waves (2, 3), Alfvén waves (11, 12), amplified magnetic tension (13), or magnetic reconnection (14). However, observations of their formation process are limited, owing to insufficient resolution and sensitivity. Two observations revealed a tendency for

the presence of opposite-polarity magnetic flux near magnetic field concentrations during the occurrence of some spicules (15, 16). However, further analysis did not yield an obvious association between spicules and magnetic field evolution (16).

We observed spicules (fig. S1) using the 1.6-m Goode Solar Telescope (GST) (17, 18) at the Big Bear Solar Observatory (BBSO). We performed Hα wing observations and simultaneous magnetic flux measurements with GST's Near Infra-Red Imaging Spectropolarimeter (NIRIS) (19). NIRIS enables us to obtain information on photospheric magnetic fields by spectropolarimetric observations of the Fe I 1.56 µm line (18) (figs. S2 and S3). Figure 1A shows a solar image at the blue wing (-0.8 Å from line core)of the $H\alpha$ line. It is dominated by numerous elongated dark jets, i.e., spicules. These spicules mostly originate from the magnetic network, indicated by the locations of magnetic field concentrations with positive polarity (Figs. 1 and S2).

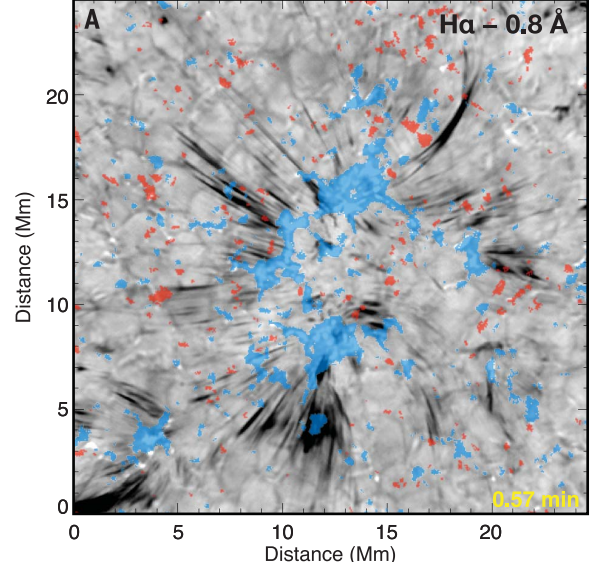
In addition to frequent individual spicules, occasionally several spicules originate simultaneously from a small region, appearing as enhanced spicular activity at a single location (movie S1). These enhanced spicular activities are accompanied by the presence of weak magnetic elements with a polarity opposite to the dominant polarity of the magnetic

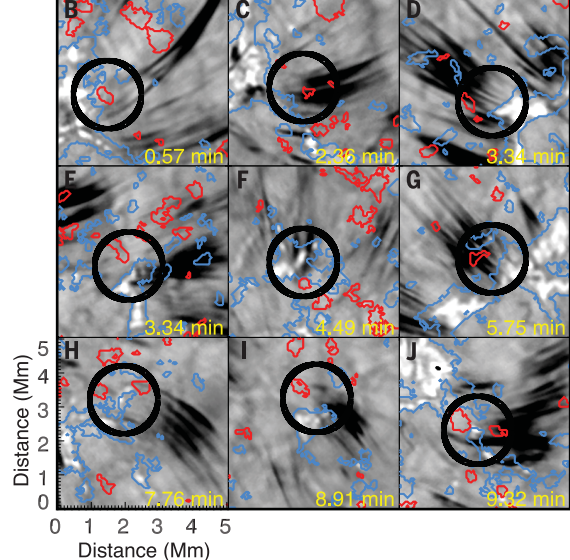
¹School of Earth and Space Sciences, Peking University, Beijing 100871, People's Republic of China. ²Big Bear Solar Observatory, New Jersey Institute of Technology, 40386 North Shore Lane, Big Bear City, CA 92314-9672, USA. ³Max Planck Institute for Solar System Research, Justus-von-Liebig-Weg 3, D-37077 Göttingen, Germany. ⁴NASA Marshall Space Flight Center, Huntsville, AL 35812, USA. ⁵Solar Physics and Space Plasma Research Centre, School of Mathematics and Statistics, University of Sheffield, Hounsfield Road, Sheffield S3 7RH, UK. ⁶Department of Astronomy, Eötvös Loránd University, Budapest, H-1117 Budapest, Hungary. ⁷Faculty of Information Engineering and Automation, Kunming University of Science and Technology, Kunming 650500, People's Republic of China. ⁸Institute for Geophysics, Astrophysics and Meteorology–Institute of Physics, University of Graz, Universitätsplatz 5, 8010 Graz, Austria. ⁹Indian Institute of Astrophysics, Koramangala, Bangalore 560034, India.

*Corresponding author. Email: huitian@pku.edu.cn

Fig. 1. Association of enhanced spicular activities with opposite-polarity magnetic fields.

(A) $H\alpha$ blue wing image (gray-scale) overlain with a binary magnetic field map shown in blue and red, representing longitudinal flux densities of at least +10 Mx cm⁻² and -10 Mx cm⁻², respectively (1 Mx = 10⁻⁸ Wb; the unit of Mx cm⁻² is equivalent to Gauss). Movie S1 shows an animated version of this panel. Figure S1 shows the





location of this region, and observational parameters are listed in table S1. (**B** to **J**) Examples of enhanced spicular activities. Blue and red contours outline regions of ± 10 Mx cm⁻² for the longitudinal flux density. Axes are the same in different panels. The black circle (with a radius of 1 Mm) in each panel highlights a region around the footpoint of a region of enhanced spicular activity, where at least one small negative-polarity magnetic element is observed in each case.

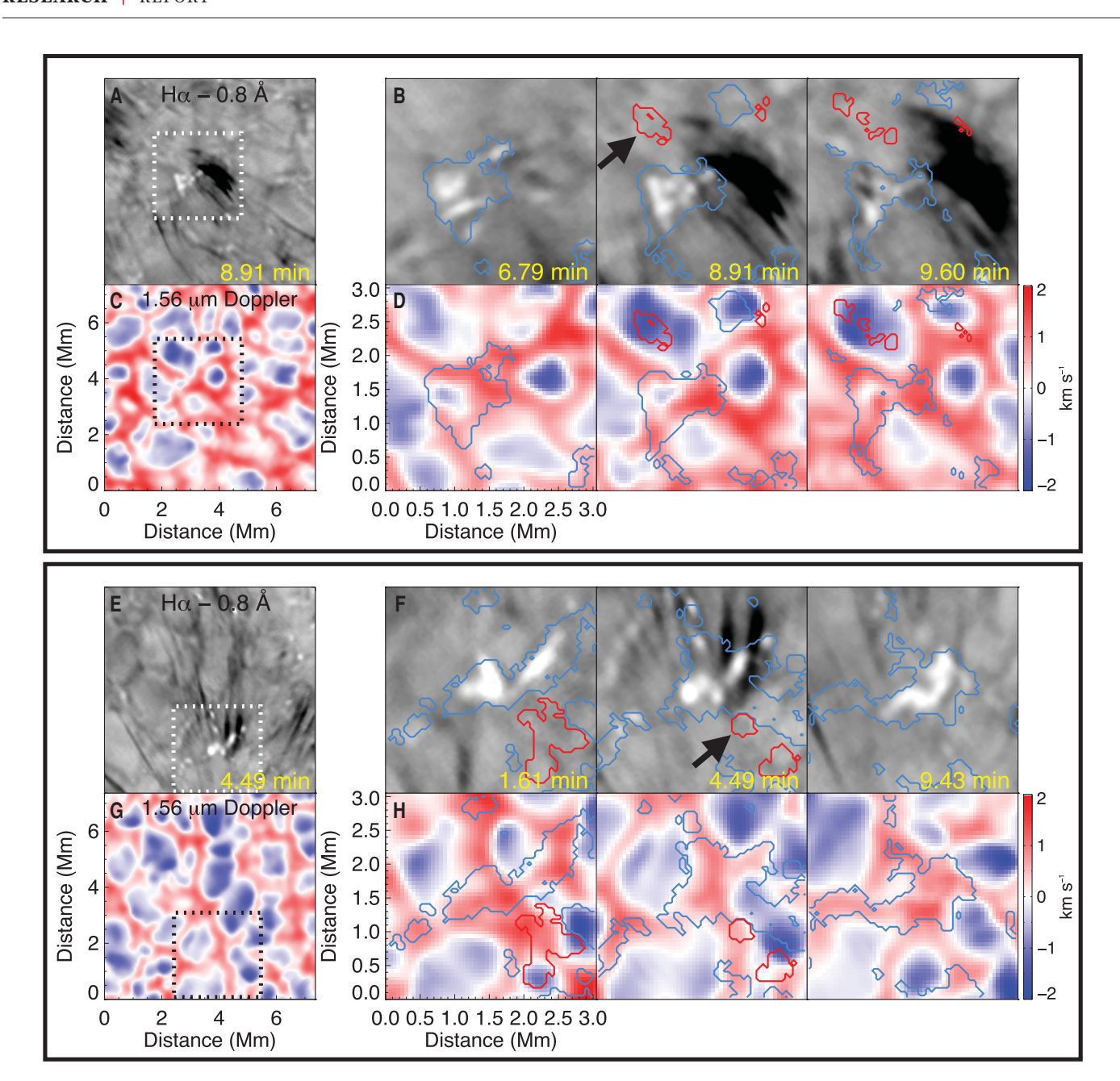


Fig. 2. Enhanced spicular activity triggered by flux emergence (A to D) (movie S2) and flux cancellation (E to H) (movie S3). (A) Enhanced spicular activity in a $H\alpha$ blue wing image. (C) Photospheric Doppler shift pattern of the same region. (B and D) Temporal evolution around the spicule footpoint region [dotted boxes in (A) and (C)]. Contour colors and levels are the same as in Fig. 1B. The arrow in (B) indicates the presence of an opposite-polarity flux. Panels (E) to (H) are the same as (A) to (D) but for a different region.

network around their footpoints (Fig. 1, B to J). When spicules occur, these weak elements are typically within several hundred kilometers from the edge of the strong network fields. By contrast, the strong and evolving unipolar fields (present for a much longer time in the network) generally do not produce enhanced spicular activities.

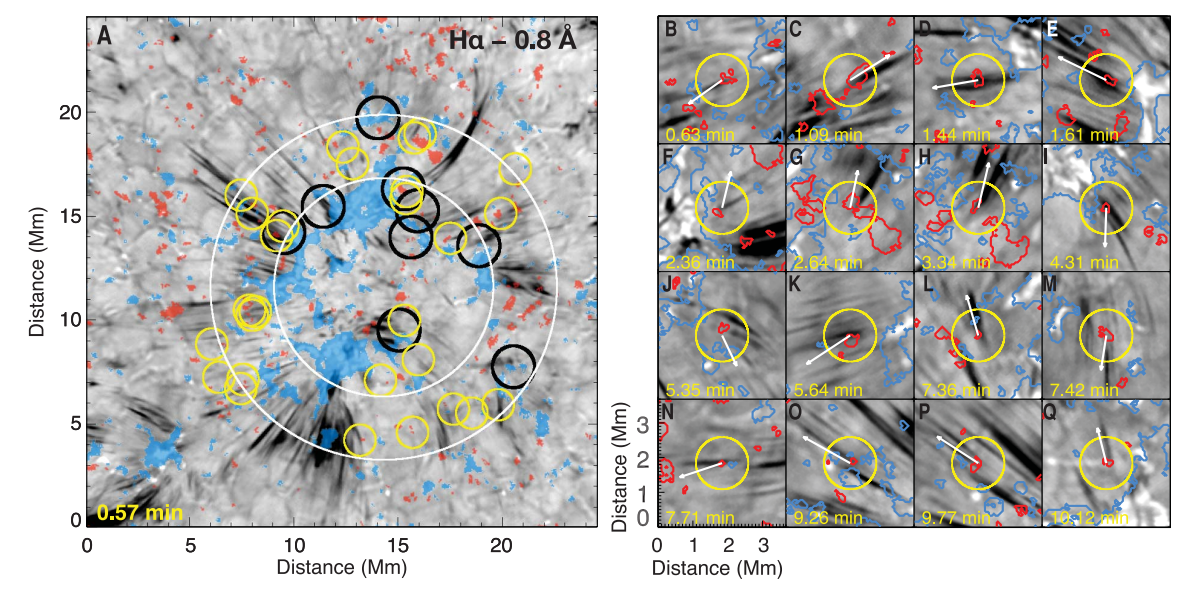
These enhanced spicular activities appear to be driven by the dynamical interaction of magnetic fields, often preceded by new flux emergence or appearance, and sometimes accompanied by apparent flux cancellation near the network edge. Figure 2, A to D, shows a patch of small-scale weak field with negative polarity that emerges near the strong positive-polarity network fields in the photosphere. Its coincidence with a patch of large blue shift of Fe $\scriptstyle\rm I$ also indicates the emergence of the field (movie S2 and figs. S4 and S5). This flux emergence is followed within minutes by enhanced spicular activity, observed in the blue wing of H α . Figure 2, E to H, shows a larger patch of weak negative-polarity field

that approaches the strong network fields; the subsequent flux cancellation leads to enhanced spicular activity (movie S3). The flux cancellation takes place at the boundary of a convection cell that is characterized by red shifts of the Fe $_{\rm I}$ line.

Almost all the enhanced spicular activities that we observed are associated with emergence or appearance of negative-polarity fluxes and/or subsequent flux cancellation around the boundary of the positive-polarity magnetic network (Figs. 2 and S6 and movie S4). Furthermore,

Fig. 3. Connection of individual spicules to opposite-polarity magnetic fluxes.

(A) The same image as Fig. 1A, overlain with an inner white circle (a radius of 5.25 Mm) representing the approximate boundary of the network, and an outer white circle 3 Mm outside it. Black circles mark the footpoint regions of the same regions with enhanced spicular activity as shown in Fig. 1, B to J. Yellow circles have a radius of 0.75 Mm and indicate regions shown in (B) to (Q) and in fig. S7, which



mostly lie within the outer white circle. Movie S4 shows an animated version of this panel. (\mathbf{B} to \mathbf{Q}) Sixteen examples showing the presence of an opposite-polarity flux near the spicule footpoint (indicated by the yellow circles). Contour colors and levels are the same as in Fig. 1B. The white arrow in each panel indicates the direction radially outward from the center of the white circles.

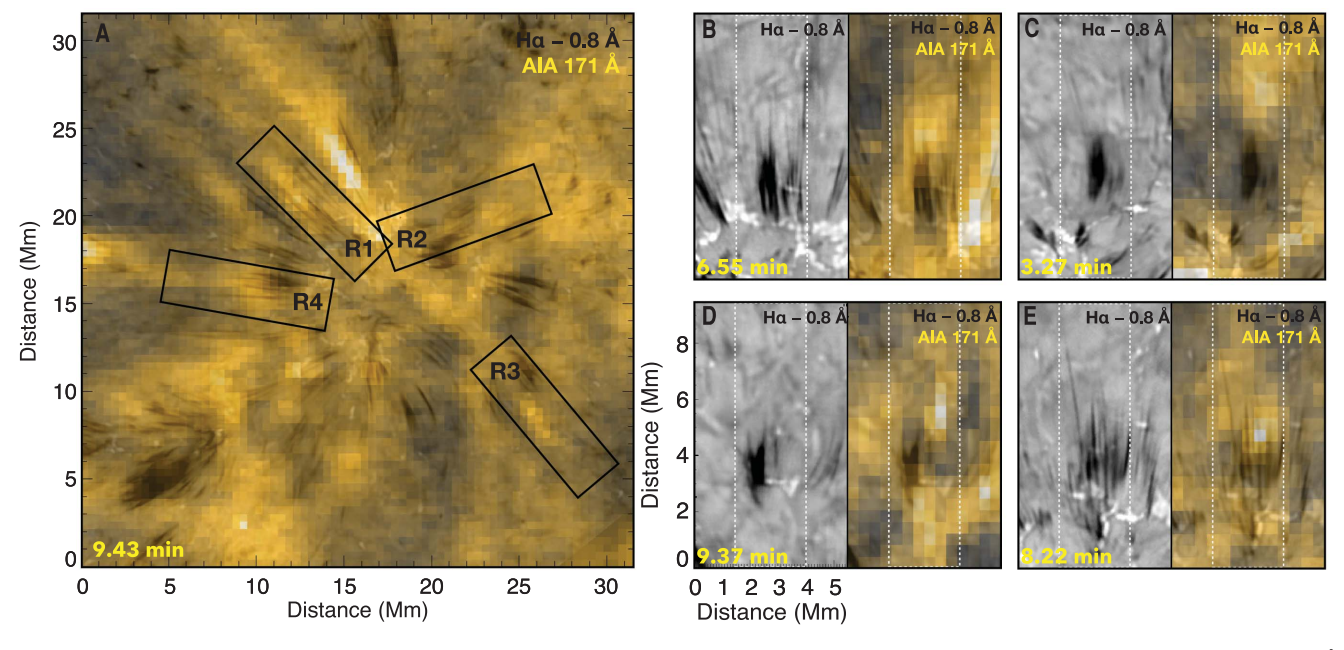


Fig. 4. Coronal connection of enhanced spicular activities (movie S5). (**A**) H α blue wing image (grayscale) overlain with the simultaneously taken AIA 171 Å image (yellow). Boxes indicate regions shown in the other panels. (**B** to **E**) Four examples showing the enhancement of coronal emission above regions of enhanced spicular activity (more examples are in fig. S8). The H α blue wing and the same image overlain with the simultaneous AIA 171 Å image are shown in each pair of panels. The white dotted boxes in (B) to (E) correspond to the black boxes (R1 to R4) in (A), respectively.

many individual spicules appear to originate, sometimes repeatedly, from small-scale negative-polarity magnetic features located near the strong network fields (Fig. 3 and fig. S7). Although small-scale flux emerges or appears ubiquitously in the quiet Sun, our observations indicate that only when it is close to the strong network fields (often <3 Mm; Fig. 3 and movie S4) does

it generate spicules. For some small spicules, no opposite polarity is detected at their footpoints. Because the magnetograms have a spatial resolution (~150 km) about three times lower and a cadence (71 s) around 20 times slower than the H α images, there may be smaller-scale or highly dynamic fields at the footpoints of these small spicules that we cannot detect.

Our results support the hypothesis that fast spicules originate from magnetic reconnection (14, 20, 21). It is possible that a subphotospheric local dynamo mechanism (22) or magnetoconvection process (13, 23) generates weak magnetic fields close to the large-scale network fields. These small-scale weak fields may occasionally emerge into the photosphere and

rise to the chromosphere, where they could reconnect with adjacent or overlying network fields to produce spicules. Alternatively, an opposite-polarity magnetic element could appear as a result of the coalescence and concentration of previously existing dispersed and unresolved fluxes (24), then reconnect with the network fields to generate spicules.

Spicules might supply hot plasma to the solar corona (4, 5, 9). We analyzed coronal observations of the same region with the Atmospheric Imaging Assembly (AIA) (25) on the Solar Dynamics Observatory (SDO) spacecraft (18). Most of the enhanced spicular activities are seen to channel hot plasma into the corona (Fig. 4, figs. S8 and S9, and movies S5 to S8). Coronal emission (visible in AIA images at 171 Å) generally appears at the top of the spicules. Our observations in a quiet-Sun region (fig. S1) complement previous observations (4, 26) that identified similar coronal signatures for some chromospheric upflow events observed above the solar limb or in on-disk active regions (regions around sunspots). Our observations reveal that magnetic reconnection events at network boundaries can drive spicules and produce hot plasma flows into the corona, providing a link between magnetic activities in the lower atmosphere and coronal heating. It remains unclear whether this process can provide sufficient heating to explain the high temperature of the corona (27, 28).

Heated material sometimes falls back from the corona (fig. S10 and movie S9), which could be responsible for the prevalent redshifts of emission lines formed in the chromospherecorona transition region (29, 30). Our observa-

tions of the formation of spicules, the subsequent heating, and the return flows reveal a complete mass cycling process between the chromosphere and corona.

REFERENCES AND NOTES

- 1. J. M. Beckers, Annu. Rev. Astron. Astrophys. 10, 73-100
- A. C. Sterling, Sol. Phys. 196, 79-111 (2000).
- B. De Pontieu, R. Erdélyi, S. P. James, Nature 430, 536-539 (2004)
- 4. B. De Pontieu et al., Science 331, 55-58 (2011).
- R. G. Athay, T. E. Holzer, Astrophys. J. 255, 743 (1982).
- G. Tsiropoula et al., Space Sci. Rev. 169, 181-244 (2012).
- B. De Pontieu et al., Publ. Astron. Soc. Jpn. 59 (sp3), S655-S652 (2007)
- 8 | Rouppe van der Voort | Leenaarts B de Pontieu M. Carlsson, G. Vissers, Astrophys. J. 705, 272-284 (2009)
- 9. H. Tian et al., Science 346, 1255711 (2014).
- 10. T. M. D. Pereira et al., Astrophys. J. 792, L15 (2014).
- 11. S. R. Cranmer, L. N. Woolsey, Astrophys. J. 812, 71 (2015).
- 12. H. lijima, T. Yokovama, Astrophys, J. 848, 38 (2017).
- 13. J. Martínez-Sykora et al., Science 356, 1269-1272 (2017).
- 14. J. Y. Ding et al., Astron. Astrophys. 535, A95 (2011). 15. V. Yurchyshyn, V. Abramenko, P. Goode, Astrophys. J. 767, 17
- (2013).
- 16. N. Deng et al., Astrophys. J. 799, 219 (2015)
- 17. W. Cao et al., Astron. Nachr. 331, 636-639 (2010)
- 18. Materials and methods are available as supplementary materials
- 19. W. Cao et al., Astron. Soc. Pac. Conf. Ser. 463, 291 (2012).
- 20. R. L. Moore, A. C. Sterling, J. W. Cirtain, D. A. Falconer, Astrophys. J. 731, L18 (2011).
- 21. A. C. Sterling, R. L. Moore, Astrophys. J. 828, L9 (2016).
- 22. T. Amari, J.-F. Luciani, J.-J. Aly, Nature 522, 188-191 (2015).
- 23. F. Moreno-Insertis, J. Martínez-Sykora, V. H. Hansteen, D. Muñoz Astrophys. J. 859, L26 (2018).
- 24. D. A. Lamb, C. E. DeForest, H. J. Hagenaar, C. E. Parnell,
- B. T. Welsch, Astrophys. J. 674, 520–529 (2008). 25. J. R. Lemen et al., Sol. Phys. 275, 17-40 (2012).
- 26. H. Ji, W. Cao, P. R. Goode, Astrophys. J. 750, L25 (2012).
- 27. J. A. Klimchuk, J. Geophys. Res. 117 (A12), A12102 (2012).
- 28. M. L. Goodman, Astrophys. J. 785, 87 (2014).
- 29. H. Peter, P. G. Judge, Astrophys. J. 522, 1148-1166 (1999).
- 30. S. W. McIntosh, H. Tian, M. Sechler, B. De Pontieu, Astrophys. J. 749, 60 (2012).

ACKNOWLEDGMENTS

BBSO operation is supported by NJIT and NSF. GST operation is partly supported by the Korea Astronomy and Space Science Institute (KASI); Seoul National University; the Strategic Priority Research Program of CAS (grant no. XDB09000000); and the Operation, Maintenance and Upgrading Fund for Astronomical Telescopes and Facility Instruments administrated by CAS. The AIA is an instrument on SDO, a mission of NASA's Living With a Star Program. We thank the GST and SDO teams for providing the data and S. K. Solanki and L. R. Bellot Rubio for helpful discussion. Funding: This work is supported by NSFC grants 11825301, 11790304(11790300), 41574166, 11729301, U1931107, and 11850410435; NSF grants AGS 1821294, 1620875, and AST-1614457; AFOSR grant FA9550-19-1-0040, NASA grants HGC 80NSSC17K0016 and HGI 17-HGISUN17_2-0047; Max Planck Partner Group program, Strategic Priority Research Program of CAS (grant XDA17040507), Key Applied Basic Research Program of Yunnan Province (FS: 2018FA035), FWF project N27800, CAS Presidents International Fellowship Initiative grant no. 2019VMA052, UK STFC grant ST/M000826/ 1, and the Royal Society. Author contributions: H.T. and T.S. conceived the study and wrote the manuscript, T.S. analyzed the data and generated the figures and movies under H.T.'s guidance. V.Y. generated the GST observations, processed the GST data, and advised on the data analysis. W.C. developed instruments on GST. K.A. processed the GST NIRIS data for scientific use. S.F. helped co-align the data. Y.C. performed the energy calculation and helped verify the results. H.P., A.S., R.E., D.U., and D.B. contributed to the interpretation of the observations. All authors discussed the results and commented on the manuscript. Competing interests: There are no competing interests. Data and materials availability: The GST dataset that we used is available at http://ftp.bbso.njit. edu/pub/20170619/. The AIA data are available at the Joint Science Operations Center, http://jsoc.stanford.edu/AIA/ AIA_lev1.html; we used the 12 s 171 Å and 24 s 1700 Å observations in the time range 2017 June 19 18:45-18:57 UT.

SUPPLEMENTARY MATERIALS

science.sciencemag.org/content/366/6467/890/suppl/DC1 Materials and Methods

Supplementary Text

Figs. S1 to S10

Table S1

References (31-88)

Movies S1 to S9

4 December 2018: accented 24 October 2019 10.1126/science.aaw2796



Generation of solar spicules and subsequent atmospheric heating

Tanmoy Samanta, Hui Tian, Vasyl Yurchyshyn, Hardi Peter, Wenda Cao, Alphonse Sterling, Robertus Erdélyi, Kwangsu Ahn, Song Feng, Dominik Utz, Dipankar Banerjee and Yajie Chen

Science 366 (6467), 890-894. DOI: 10.1126/science.aaw2796

Magnetic fields can generate spicules
Spicules are small jets of plasma from the surface of the Sun that last a few minutes. Around a million are occurring at any moment, even during periods of low solar activity. The mechanism responsible for launching spicules remains unknown, as is their contribution to heating the solar corona. Samanta et al. observed emerging spicules and the magnetic fields in the adjacent solar surface. They found that many spicules appear a few minutes after a patch of reverse-polarity magnetic field and that the overlying corona is heated shortly afterward. This result provides evidence that magnetic reconnection can generate spicules, which then transfer energy to the corona.

Science, this issue p. 890

ARTICLE TOOLS http://science.sciencemag.org/content/366/6467/890

SUPPLEMENTARY MATERIALS http://science.sciencemag.org/content/suppl/2019/11/13/366.6467.890.DC1

RELATED CONTENT file:/content

REFERENCES This article cites 88 articles, 5 of which you can access for free

http://science.sciencemag.org/content/366/6467/890#BIBL

PERMISSIONS http://www.sciencemag.org/help/reprints-and-permissions

Use of this article is subject to the Terms of Service

Science (print ISSN 0036-8075; online ISSN 1095-9203) is published by the American Association for the Advancement of Science, 1200 New York Avenue NW, Washington, DC 20005. The title Science is a registered trademark of AAAS.